PHYSICAL REVIEW D **92,** 074505 (2015)

Landau gauge ghost propagator and running coupling in $SU(2)$ lattice gauge theory

V. G. Bornyakov
Institute for High Energy Physics NRC "Kurchatov Institute", 142281 Protvino, Russia, Institute of Theoretical and Experimental Physics, 117259 Moscow, Russia, and School of Biomedicine, Far Eastern Federal University, 690950 Vladivostok, Russia

E.-M. Ilgenfritz
Joint Institute for Nuclear Research, BLTP, 141980 Dubna, Russia

C. Litwinski and M. Müller-Preussker
Humboldt-Universität zu Berlin, Institut für Physik, 12489 Berlin, Germany

V. K. Mitrjushkin
Joint Institute for Nuclear Research, BLTP 141980 Dubna, Russia, and Institute of Theoretical and Experimental Physics, 117259 Moscow, Russia

(Received 13 April 2013; revised manuscript received 3 August 2015; published 20 October 2015)

We study finite (physical) volume and scaling violation effects of the Landau gauge ghost propagator as well as of the running coupling $\alpha_s(p)$ in the $SU(2)$ lattice gauge theory. We consider lattices with physical linear sizes between $aL \simeq 3$ and $aL \simeq 7$ fm and values of lattice spacing between $a = 0.2$ and $a = 0.07$ fm. To fix the gauge we apply an efficient gauge fixing method aimed at finding extrema as close as possible to the global maximum of the gauge functional. We find finite volume effects to be small for the lattice size $aL \simeq 3$ fm at momenta $|p| \gtrsim 0.6$ GeV. For the same lattice size we study extrapolations to the continuum limit of the ghost dressing function as well as for the running coupling with momenta chosen between $|p| = 0.41$ and $|p| = 3.2$ GeV. We present fit formulas for the continuum limit of both observables in this momentum range. Our results testify in favor of the decoupling behavior in the infrared limit.

DOI: 10.1103/PhysRevD.92.074505 PACS numbers: 11.15.Ha, 12.38.Aw, 12.38.Gc

I. INTRODUCTION

The infrared (IR) behavior of Landau gauge gluon and ghost propagators is believed to be closely related to gluon and quark confinement. The celebrated Gribov-Zwanziger/Kugo-Ojima (GZKO) color confinement scenario [1–5] has prescribed that the gluon propagator $D(p)$ should vanish in the IR limit $p \to 0$ (the so-called infrared suppression), while the ghost dressing function $p^2G(p)$ was expected to become singular in this limit (infrared enhancement).

The search for gluon and ghost propagator solutions of Dyson-Schwinger (DS) and functional renormalization group (FRG) equations showed the existence of infrared solutions exhibiting a powerlike *scaling* behavior [6–14]. Later also regular so-called *decoupling* solutions providing an IR-finite limit of both the gluon propagator and the ghost dressing function [15–19] have been found. Both kinds of solutions can be realized by different IR boundary conditions for the ghost dressing function as it has been argued in [20]. As one understood immediately, both of them can support quark confinement [21], and the gluon propagator breaks reflection positivity. The decoupling solution cannot be reconciled with the GZKO scenario. However, it is in agreement with the refined Gribov-Zwanziger formalism developed in Refs. [22,23].

From the phenomenological point of view the propagators can serve as input to bound state equations as there are Bethe-Salpeter or Faddeev equations for hadron phenomenology [8,24,25]. In the ultraviolet limit they allow a determination of phenomenogically relevant parameters such as $\Lambda_{\overline{\mathrm{MS}}}$ or condensates $\langle\bar{\psi}\psi\rangle, \langle A^2\rangle, \ldots$, by fitting *ab initio* lattice data to continuum expressions (see e.g. [26,27] and references therein) obtained from operator product expansion and perturbation theory [28,29].

What concerns the solution of DS and/or FRG equations it is well known that in practice the system of those equations is truncated. The details of truncation influence the behavior of the Green functions especially in the nonperturbative momentum range around 1 GeV, where the Landau gauge gluon dressing function exhibits a pronounced maximum. Therefore, reliable results from *ab initio* lattice computations to compare with or even used as an input for DS or FRG equations are highly welcome.

On the lattice, over almost 20 years extensive studies of the Landau gauge gluon and—in the present paper discussed again—ghost propagators have been carried out

 © 2015 American Physical Society

(see, e.g., [30–51]). A serious problem in these calculations represents the ambiguity of Landau gauge fixing (the Gribov copy problem) [52–61]. As long as the latter is solved by extremizing the Landau gauge functional (for alternative approaches see [62,63]) numerical lattice results clearly support the decoupling type of solutions in the IR limit and the lack of IR enhancement of the ghost propagator [43,44,47,49,51,58]. For the gluon propagator Zwanziger recently has derived a strict bound $\lim_{p\to 0} p^{d-2}D(p) = 0$ also allowing $D(0) \neq 0$ for $d > 2$ [64], i.e. a decoupling behavior (see also [65]). Note that for such a behavior it became more and more evident that BRST symmetry is broken [66–69].

However, most of the lattice computations dealing with the IR limit were relying on rather coarse lattices in order to reach large enough volumes. A systematic investigation of lattice discretization artifacts or scaling violations and an extrapolation to the continuum was missing for quite a long time.

In this paper we present an investigation for the ghost dressing function and—employing previous gluon propagator results [70]—obtain the running coupling within the so-called minimal momentum subtraction (MOM) scheme [71]. We restrict ourselves to the $SU(2)$ case of pure gauge theories, having in mind the close similarity to the more realistic $SU(3)$ case as observed in [45,46].

We shall use the same lattice field configurations as in [70] which were gauge fixed with an improved method taking into account many copies over all $Z(2)$ Polyakov loop sectors and applying simulated annealing with subsequent overrelaxation. We separately discuss the case of fixed lattice spacing and varying volume (from $aL \simeq 3$ to $aL \simeq 7$ fm) and the case of fixed physical volume and varying lattice spacing (between $a = 0.21$ and $a = 0.07$ fm). In the range of IR momenta achieved in this setting, finite-size effects are shown to be negligibly small. But relative finite-discretization effects in the infrared (for a renormalization scale chosen at $\mu = 2.2$ GeV) turn out to be more sizable and can be quantified to reach a 10 percent variation level at $p \simeq 0.4$ GeV in the approximate scaling region explored between $\beta = 2.3$ and $\beta = 2.55$. A similar observation can be made for the running coupling. Therefore, a careful analysis of the lattice artifacts is mandatory. We carry out such an analysis by taking the continuum limit extrapolations (for the first time to our knowledge) for the ghost propagator as well as for the running coupling for selected physical momentum values in the range from $|p| = 0.41$ to $|p| = 3.2$ GeV. The continuum extrapolated values can then be fitted with appropriate formulas describing a smooth continuum behavior of the observables in the given momentum range.

In Sec. II we introduce the lattice Landau gauge and the corresponding Faddeev-Popov operator and the ghost propagator. In Sec. III some details of the simulation and of the improved gauge fixing are repeatedly given for the convenience of the reader. In Sec. IV we present our numerical results for the ghost propagator and the running coupling. Conclusions will be drawn in Sec. V.

II. LATTICE LANDAU GAUGE AND THE GHOST PROPAGATOR

Let us briefly recall how the $SU(2)$ gauge field configurations used in Ref. [70] for measuring the gluon propagator have been created and gauge fixed.

The non-gauge-fixed $SU(2)$ gauge field configurations were generated with a standard Monte Carlo routine using the standard plaquette Wilson action

$$S = \beta \sum_x \sum_{\mu>\nu} \left[1 - \frac{1}{2} \mathrm{Tr}\left(U_{x\mu} U_{x+\hat{\mu};\nu} U^\dagger_{x+\hat{\nu};\mu} U^\dagger_{x\nu} \right) \right],$$
$$\beta = 4/g_0^2, \tag{1}$$

where g_0 denotes the bare coupling constant. The link variables $U_{x\mu} \in SU(2)$ transform under local gauge transformations g_x as follows:

$$U_{x\mu} \overset{g}{\mapsto} U^g_{x\mu} = g^\dagger_x U_{x\mu} g_{x+\hat{\mu}}, \qquad g_x \in SU(2). \tag{2}$$

The standard (linear) definition [30] for the dimensionless lattice gauge vector potential $\mathcal{A}_{x+\hat{\mu}/2,\mu}$ is

$$\mathcal{A}_{x+\hat{\mu}/2,\mu} = \frac{1}{2i}(U_{x\mu} - U^\dagger_{x\mu}) \equiv A^a_{x+\hat{\mu}/2;\mu} \frac{\sigma_a}{2}. \tag{3}$$

The definition of the gluon field is not unique at finite a, which may influence the propagator results in the IR region, where the continuum limit is more difficult to control.

In lattice gauge theory the most natural choice of the Landau gauge condition is by transversality [30]

$$(\partial\mathcal{A})_x = \sum_{\mu=1}^{4} (\mathcal{A}_{x+\hat{\mu}/2;\mu} - \mathcal{A}_{x-\hat{\mu}/2;\mu}) = 0, \tag{4}$$

which is equivalent to finding a local extremum of the gauge functional

$$F_U(g) = \frac{1}{4V} \sum_{x\mu} \frac{1}{2} \mathrm{Tr} U^g_{x\mu} \tag{5}$$

with respect to gauge transformations g_x. $V = L^4$ denotes the $4d$ lattice size.The Gribov ambiguity is reflected by the existence of multiple local extrema. The manifold consisting of Gribov copies providing local maxima of the functional (5) and a semipositive Faddeev-Popov operator (see below) is called the *Gribov region* Ω, while the global maxima form what is called the *fundamental modular region* $\Lambda \subset \Omega$. Our gauge fixing procedure is aiming to

approach Λ by finding higher and higher maxima. This is achieved by use of the effective optimization algorithm and finding a large number of local maxima of which the highest is picked up.

The lattice expression of the Faddeev-Popov operator M^{ab} corresponding to $M^{ab} = -\partial_\mu D_\mu^{ab}$ in the continuum theory (where D_μ^{ab} is the covariant derivative in the adjoint representation) is given by [31,72]

$$M_{xy}^{ab} = \sum_\mu \{(\bar{S}_{x\mu}^{ab} + \bar{S}_{x-\hat{\mu};\mu}^{ab})\delta_{x;y} - (\bar{S}_{x\mu}^{ab} - \bar{A}_{x\mu}^{ab})\delta_{y;x+\hat{\mu}} - (\bar{S}_{x-\hat{\mu};\mu}^{ab} + \bar{A}_{x-\hat{\mu};\mu}^{ab})\delta_{y;x-\hat{\mu}}\}, \tag{6}$$

where

$$\bar{S}_{x\mu}^{ab} = \delta^{ab}\frac{1}{2}\mathrm{Tr}U_{x\mu}, \qquad \bar{A}_{x\mu}^{ab} = -\frac{1}{2}\epsilon^{abc}A_{x+\hat{\mu}/2;\mu}^{c}. \tag{7}$$

From the form (7) it follows that a trivial zero eigenvalue is always present, such that at the Gribov horizon $\partial\Gamma$ the first nontrivial zero eigenvalue appears. For configurations with a constant field, with $b_{x\mu}^0 = \bar{b}_\mu^0$ and $b_{x\mu}^a = \bar{b}_\mu^a$ independent of x, there exist eigenmodes of M with a vanishing eigenvalue. Thus, if the Landau gauge is properly implemented, $M[U]$ is a symmetric and semipositive definite matrix.

The ghost propagator $G^{ab}(x,y)$ is defined as [31,72]

$$G^{ab}(x,y) = \delta^{ab}G(x-y) \equiv \langle (M^{-1})_{xy}^{ab}[U]\rangle, \tag{8}$$

where $M[U]$ is the Faddeev-Popov operator, on the sector orthogonal to the strict zero modes. Note that the ghost propagator becomes translationally invariant (i.e., dependent only on $x-y$) and diagonal in color space only in the result of averaging over the ensemble of gauge-fixed representatives of the original gauge-unfixed Monte Carlo gauge ensemble.

$M[U]$ can be inverted with a conjugate-gradient method, provided that both the source $\psi^a(y)$ and the initial guess for the solution are orthogonal to the zero modes. For the source we adopt the one proposed in [52] and also used in [53]:

$$\psi^a(y) = \delta^{ac}e^{2\pi i p\cdot y} \qquad p \neq (0,0,0,0), \tag{9}$$

for which the condition $\sum_y \psi^a(y) = 0$ is automatically imposed. Only the scalar product of $M^{-1}\psi$ with the source ψ itself has to be evaluated. The inversion of M is done on sources for fixed $c = 1,\ldots,3$ and the (adjoint) color averaging will be explicitly performed.

The ghost propagator in momentum space can be written as

$$G(p) = \frac{1}{3V}\sum_{x,y} e^{-2\pi i p\cdot(x-y)}\langle (M^{-1})_{xy}^{aa}[U]\rangle, \tag{10}$$

TABLE I. Values of β, lattice sizes, number of configurations and number of gauge copies used throughout Ref. [70] and this paper. The lattice spacing was fixed to its physical value using the string tension $\sqrt{\sigma} = 440$ MeV (see [73,74]).

β	a^{-1} [GeV]	a [fm]	L	aL [fm]	N_{conf}	N_{copy}
2.20	0.938	0.210	14	2.94	400	48
2.30	1.192	0.165	18	2.97	200	48
2.40	1.654	0.119	26	3.09	200	48
2.50	2.310	0.085	36	3.06	400	80
2.55	2.767	0.071	42	2.98	200	80
2.20	0.938	0.210	24	5.04	400	48
2.30	1.192	0.165	30	4.95	400	48
2.40	1.654	0.119	42	5.00	200	80
2.30	1.192	0.165	44	7.26	200	80

where the coefficient $\frac{1}{3V}$ is taken for a full normalization, including the indicated color average over $a = 1,\ldots,3$. In what follows we will denote the (bare) ghost dressing function as

$$J(p) \equiv p^2 G(p). \tag{11}$$

III. DETAILS OF THE COMPUTATION

The Monte Carlo (MC) simulations had been carried out at several β-values between $\beta = 2.2$ and $\beta = 2.55$ for various lattice sizes L. Consecutive configurations (considered to be statistically independent) were separated by 100 sweeps, each sweep consisting of one local heatbath update followed by $L/2$ microcanonical updates. In Table I we provide the full information about the field ensembles used in this investigation. The corresponding results concerning the gluon propagator have been published in [70].

The gauge fixing is completed by the $Z(2)$ flip operation as discussed in [57,75]. For the convenience of the reader we briefly recall the main features. The method consists in flipping all link variables $U_{x\mu}$ attached and orthogonal to a selected $3d$ plane by multiplying them with $-1 \in Z(2)$. Such global flips are equivalent to nonperiodic gauge transformations. They represent an exact symmetry of the pure gauge action. The Polyakov loops in the direction of the chosen links and averaged over the orthogonal $3d$ plane (base space) obviously change their sign. Therefore, the flip operations combine the 2^4 distinct gauge orbits (or Polyakov loop sectors) related to strictly periodic gauge transformations into a single large gauge orbit.

The second ingredient is the simulated annealing (SA) method, which has been investigated independently and found computationally more efficient than the exclusive use of standard overrelaxation (OR) [75–77]. The SA algorithm generates gauge transformations $g(x)$ by MC iterations with a statistical weight proportional to $\exp(4VF_U[g]/T)$. The "gauge temperature" T is an auxiliary parameter which is gradually decreased (during gauge fixing a

configuration) in order to guide the gauge functional $F_U[g]$ towards a maximum, despite its fluctuations. In the beginning, T has to be chosen sufficiently large in order to allow rapidly traversing the configuration space of $g(x)$ fields in large steps. As in Ref. [75] we have chosen $T_{\rm init} = 1.5$. After each quasiequilibrium sweep (that includes both heatbath and microcanonical updates) T has been decreased in equidistant steps. The final SA temperature has been chosen according to the requirement that during the subsequent execution of the OR algorithm the violation of the transversality condition

$$\max_{x,a}\left|\sum_{\mu=1}^{4}(A^a_{x+\hat{\mu}/2;\mu} - A^a_{x-\hat{\mu}/2;\mu})\right| < \epsilon_{\rm lor} \tag{12}$$

decreases in a *monotonous manner* for the majority of gauge fixing trials, until finally the transversality condition (12) becomes uniformly satisfied with an $\epsilon_{\rm lor} = 10^{-7}$. Such a monotonous OR behavior is reasonably satisfied for a lower gauge temperature value $T_{\rm final} = 0.01$ [76], to be reached in the last step of SA. The number of temperature steps of SA interpolating between $T_{\rm init}$ and $T_{\rm final}$ has been chosen to be 1000 for the smaller lattice sizes and has been increased to 2000 for the lattice sizes 30^4 and bigger. The finalizing OR algorithm using the Los Alamos type overrelaxation with the overrelaxation parameter value $\omega = 1.7$ requires typically a number of iterations varying from $O(10^2)$ to $O(10^3)$ before the configuration can be considered as gauge fixed with the above-mentioned precision $\epsilon_{\rm lor}$.

In what follows we call the combined algorithm employing SA (with finalizing OR) and $Z(2)$ flips with simulated annealing (FSA) algorithm. By repeated starts of the FSA algorithm we explore each $Z(2)$ Polyakov loop sector *several times* in order to find there the best ("*bc* ") copy.[1] The total number of copies per configuration $N_{\rm copy}$ for each β-value and lattice size, generated and inspected for selecting the optimal $F_U(g)$, is indicated in Table I.

Some more details suitable to speed up the gauge fixing procedure are described in [58].

In order to suppress lattice artifacts in the propagators we followed Ref. [32] and selected the allowed lattice momenta as surviving the *cylinder cut*

$$\sum_\mu k_\mu^2 - \frac{1}{4}\left(\sum_\mu k_\mu\right)^2 \le 1. \tag{13}$$

Moreover, we have applied the "α-cut" [78] $p_\mu \le (2/a)\alpha$ for every component, in order to keep close to a linear behavior of the lattice momenta $p_\mu = (2\pi k_\mu)/(aL)$, $k_\mu \in (-L/2, L/2]$. We have chosen $\alpha = 0.5$. Obviously, this cut influences large momenta only.

[1]An alternative idea to tackle the Gribov problem has been discussed in [62,63].

We define the renormalized ghost dressing function according to momentum subtraction schemes (MOM) by

$$J_{\rm ren}(p,\mu) = \mathcal{Z}(\mu, 1/a) J(p, 1/a), \tag{14}$$

$$J_{\rm ren}(p=\mu) = 1. \tag{15}$$

In practice, we have fitted the bare dressing function $J(p, 1/a)$ with an appropriate function [see Eq. (16) below] and then used the fits for renormalizing J. Assuming that lattice artifacts are sufficiently suppressed, it has to be seen whether multiplicative renormalizability really holds in the nonperturbative regime. For this it is sufficient to prove that ratios of the renormalized (or unrenormalized) propagators obtained from different cutoff values $1/a(\beta)$ will not depend on p at least within a certain momentum interval $[p_{\rm min}, p_{\rm max}]$, where $p_{\rm max}$ should be the maximal momentum surviving all the cuts applied.

In what follows the subtraction momentum has been chosen as $\mu = 2.2$ GeV.

IV. RESULTS

A. Ghost dressing function

First let us discuss the finite volume effects for the renormalized ghost dressing function $J_{\rm ren}(p,\mu)$. The data for various volumes are presented in Fig. 1 for $\beta = 2.3$ and in Fig. 2 for $\beta = 2.4$. To present the finite volume effects in more detail we fitted the data at $\beta = 2.3$ for $aL \simeq 7$ fm and at $\beta = 2.4$ for $aL \simeq 5$ fm with a fitting function of the form

$$f_J(p) = \frac{b_1}{\hat{p}^{2\kappa}} + \frac{b_2\hat{p}^2}{1+\hat{p}^2} \tag{16}$$

with the dimensionless rescaled momentum $\hat{p} \equiv p/m_{\rm gh}$ (see Table II). This *ansatz*, while describing the data reasonably well within the given momentum range, will not be applicable in the IR limit, when we assume that $J(p)$ exhibits an inflection point and bends to a finite value $J(0)$.

In the right panels of Figs. 1 and 2, respectively, the relative deviations from the fit function are shown for $\beta = 2.3$ and $\beta = 2.4$, respectively. One can see that for both β values finite volume effects for lattices even with $aL \simeq 3$ fm are small (less than 1%) for momenta $|p| \gtrsim 0.6$ GeV.

Now let us come to the discussion of lattice artifacts. In Fig. 3 (left) we show the momentum dependence of the renormalized ghost dressing function $J_{\rm ren}(p)$ for five different lattice spacings but for (approximately) the same physical size $aL \simeq 3$ fm (for the exact values see Table I). Finite-spacing effects for $\beta = 2.2, 2.3, 2.4$ in comparison with $\beta = 2.55$ are evident. The curve shows the fit function Eq. (16) for $\beta = 2.55$ (see Table II).

For every β value we computed the ghost propagator for chosen values of the momentum in the range 0.41 GeV $\le p \le$ 3.2 GeV by interpolating the data using the function

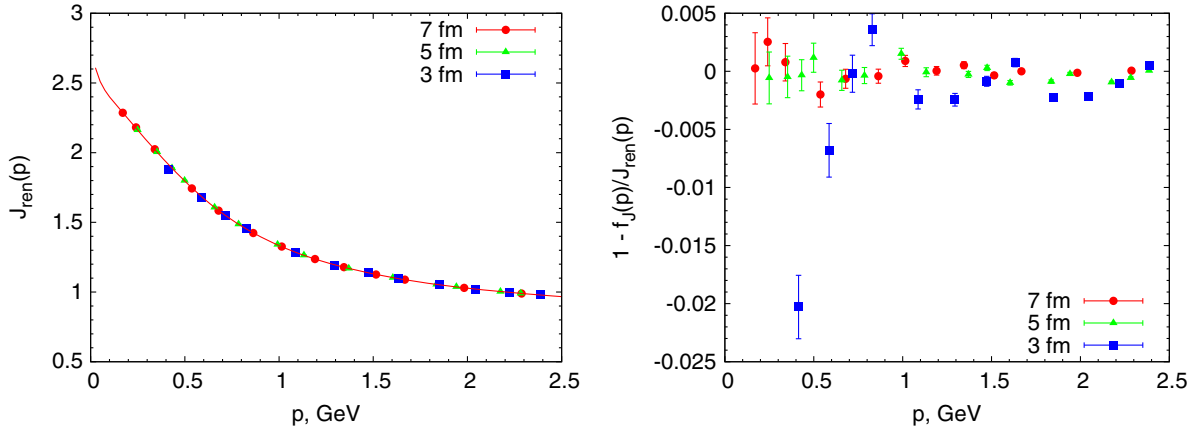

FIG. 1 (color online). Left: The momentum dependence of the renormalized ghost dressing function $J_{\rm ren}(p)$ for three different lattice sizes at $\beta = 2.3$. The curve shows the fit applying Eq. (16) to the case $aL \simeq 7$ fm. Right: The relative deviation of the data for the ghost dressing function $J_{\rm ren}(p)$ from the applied fitting curve.

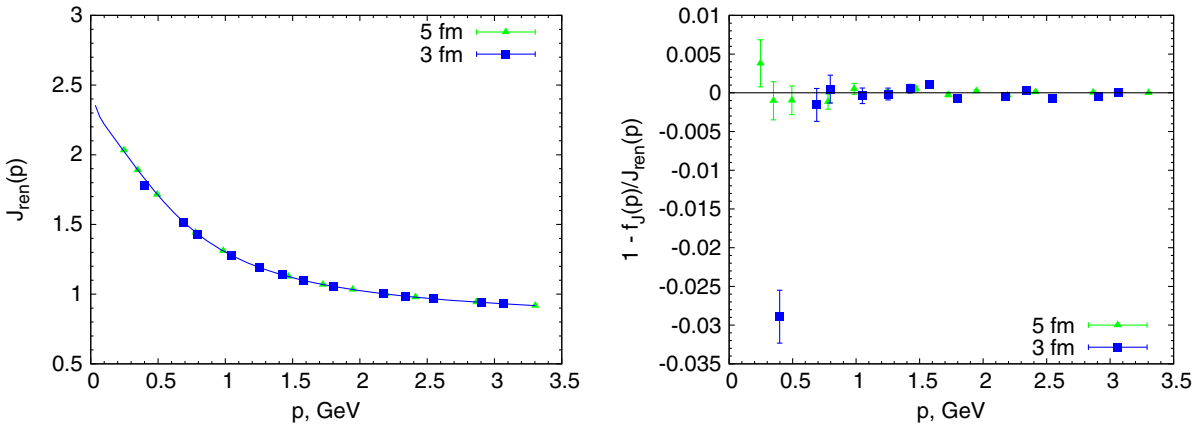

FIG. 2 (color online). The same as in Fig. 1 but for two lattice sizes at $\beta = 2.4$. The curve shows the fit applying Eq. (16) to the case $aL \simeq 5$ fm.

Eq. (16). For the interpolation four or five adjacent data points were used. For the purpose of this interpolation the choice of the function Eq. (16) was not really important. We then computed the ghost propagator in the continuum limit for these values of the momentum using a linear in a^2 extrapolation as shown in the right panel of Fig. 3. The data for the (comparably strong) coupling value $\beta = 2.2$ were not used for the extrapolation and are not shown in this figure.

TABLE II. Values of the fit parameters according to Eq. (16) and the corresponding $\chi^2_{\rm df}$. The last two lines correspond to fits of the extrapolated continuum limit values of the renormalized ghost dressing function in accordance with Eqs. (16) and (17), respectively, for lattice size $aL \simeq 3$ fm.

β	L	$m_{\rm gh}$ [GeV]	κ	b_1	b_2	$\chi^2_{\rm df}$
2.30	44	0.64(1)	0.026(1)	2.20(1)	−1.15(1)	1.8
2.40	42	0.67(1)	0.0232(4)	2.05(1)	−1.03(1)	1.9
2.55	42	0.696(15)	0.0215(4)	1.90(2)	−0.89(2)	2.27
C.L. 1		0.743(5)	0.016(1)	1.827(5)	−0.85(1)	0.07
C.L. 2		0.708(5)	0.027(1)	1.898(5)	−0.930(4)	0.04

Related to our choice of the (re)normalization momentum $\mu = 2.2$ GeV and due to the rather small statistical errors for the ghost dressing function we see clear scaling violations especially in the IR region but also for $p > \mu$. At the lowest (here accessible) momenta the violations at $\beta = 2.3$ ($\beta = 2.55$) relative to the continuum limit value are staying below 14% (3%).

Thus, in comparison with corresponding estimates for the gluon propagator (see Fig. 13 in [70]) which were more noisy, we can say that the relative scaling violations of the ghost dressing function turn out to be somewhat larger.

Similar to the case $aL \simeq 3$ fm we observe analogous lattice spacing effects on volumes with linear size $aL \simeq 5$ fm. The respective results are depicted in Fig. 4. As for the smaller volume we discard the data for $\beta = 2.2$.

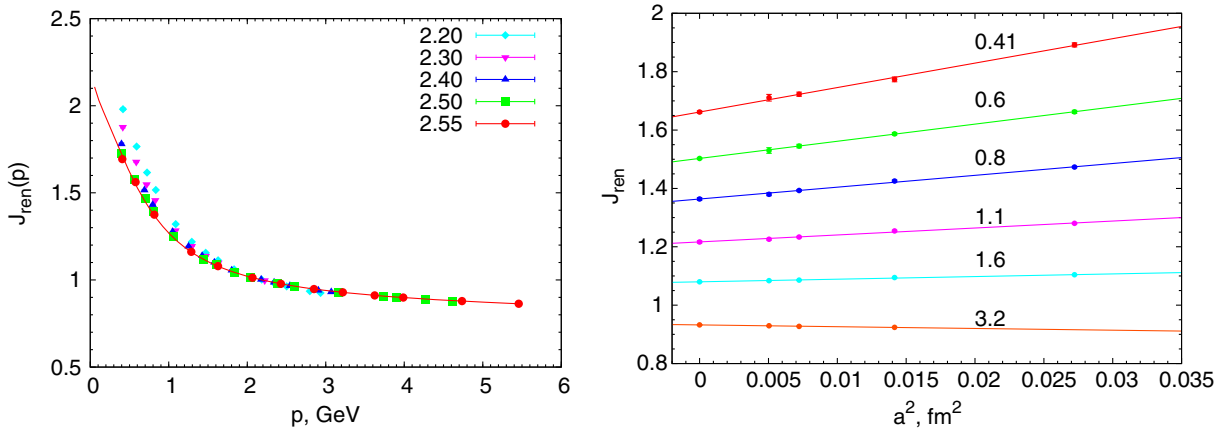

FIG. 3 (color online). Left: The momentum dependence of the renormalized ghost dressing function $J_{\rm ren}(p)$ for five different β-values or lattice spacings. The physical linear box size is $aL \simeq 3$ fm. The fitting curve belongs to the smallest available lattice spacing ($\beta = 2.55$). Right: The continuum limit extrapolation for the ghost dressing function $J_{\rm ren}(p)$. The lines show fits linear in a^2. The numbers indicate the momentum values p in GeV. Corresponding points related to $\beta = 2.2$ are not taken into account for the linear fit and, thus, not shown. The leftmost data points show the continuum extrapolated results.

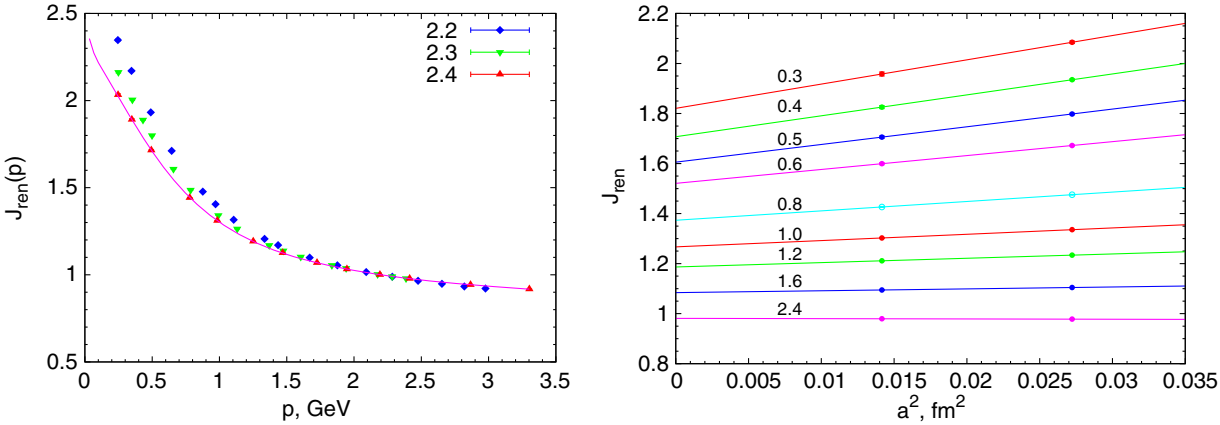

FIG. 4 (color online). Left: Same as in Fig. 3 but for a linear box size of $aL \simeq 5$ fm and three different β-values. The fitting curve belongs to $\beta = 2.40$. Right: Dressing function $J_{\rm ren}(p)$ for few selected momenta as a function of a^2. Data points related to the stronger coupling value $\beta = 2.2$ are again discarded. The straight lines are only to guide the eye.

Under these circumstances a real extrapolation to the continuum limit cannot be done. Nevertheless, Fig. 4 (right) clearly demonstrates finite lattice effects of a strength similar to the smaller volume case.

Finally, let us present the continuum extrapolated result for the smaller volume of $aL \simeq 3$ fm in Fig. 5. We show the extracted points together with two fit curves: one with the *ansatz* Eq. (16) and the other with the alternative *ansatz*

$$f_J^{(2)}(p) = b_1 + \frac{b_2 \hat{p}^2}{(1+\hat{p}^2)^{(1-\kappa)}}, \qquad \hat{p} \equiv p/m_{\rm gh}. \qquad (17)$$

This function takes a nonzero value at $p = 0$. We obtained good $\chi^2_{\rm df}$ in both cases, 0.07 and 0.04, respectively. The parameters for both fitting curves are provided in the last two lines of Table II.

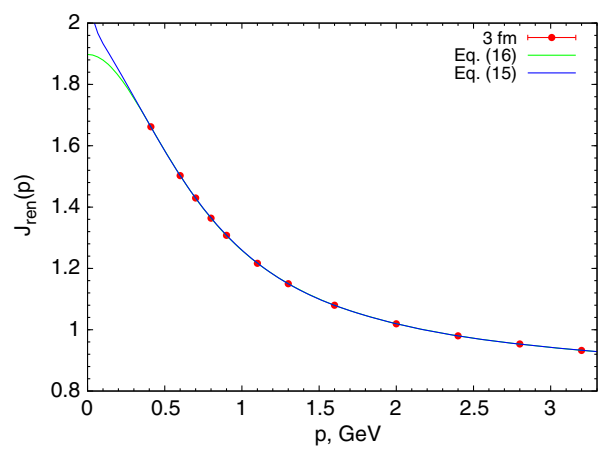

FIG. 5 (color online). The momentum dependence of the renormalized ghost dressing function $J_{\rm ren}(p)$ extracted in the continuum limit for selected momenta for $aL \simeq 3$ fm. The curves show fits with the *ansatzes* [Eqs. (16) and (17)], respectively.

TABLE III. Values of the fit parameters for α_s [Eq. (19)] and the corresponding $\chi^2_{\rm df}$. The last line collects the corresponding fit parameter values in the continuum limit extrapolated case for a linear lattice size of 3 fm.

β	L	m_α [GeV]	c_1	c_2	c_3	$\chi^2_{\rm df}$
2.30	44	1.03(1)	0.19(4)	2.3(2)	12(2)	0.95
2.40	42	1.01(1)	0.16(1)	2.63(5)	11.0(7)	0.81
2.55	42	1.04(1)	0.205(3)	2.29(3)	11.0(7)	1.3
C.L.		1.01(2)	0.199(15)	2.56(8)	10.0(1.1)	0.57

B. Running coupling

Taking the gluon dressing function results from [70] into account we can compute the minimal MOM scheme running coupling [71] via

$$\alpha_s(p) = \frac{g_0^2}{4\pi} Z(p) J(p)^2, \tag{18}$$

where $Z(p)$ and $J(p)$ are the bare gluon and ghost dressing functions, respectively.

For the running coupling we use the following dimensionless fitting function:

$$f_\alpha(p) = \frac{c_1 \hat{p}^2}{1+\hat{p}^2} + \frac{c_2 \hat{p}^2}{(1+\hat{p}^2)^2} + \frac{c_3 \hat{p}^2}{(1+\hat{p}^2)^4}, \quad \hat{p} \equiv p/m_\alpha. \tag{19}$$

The fit results for the same combinations of values (β, L) as for the ghost dressing function (see Table II) are collected in Table III.

Finite volume effects for the running coupling are shown in Fig. 6 for $\beta = 2.3$ and in Fig. 7 for $\beta = 2.4$. In both cases one can see the finite volume effects to be reasonably small (less than 5%) at a linear physical lattice extension $aL \simeq 3$ fm and for momenta $|p| \gtrsim 0.6$ GeV.

Results for the scaling check of $\alpha_s(p)$ taking into account four lattice spacings for the same extent of $aL \simeq 3$ fm are presented in Fig. 8. We see relative deviations for $\beta = 2.3$ in comparison with $\beta = 2.55$ up to a 10% level within the momentum range explored. Similar to the ghost dressing function we made extrapolations to the continuum

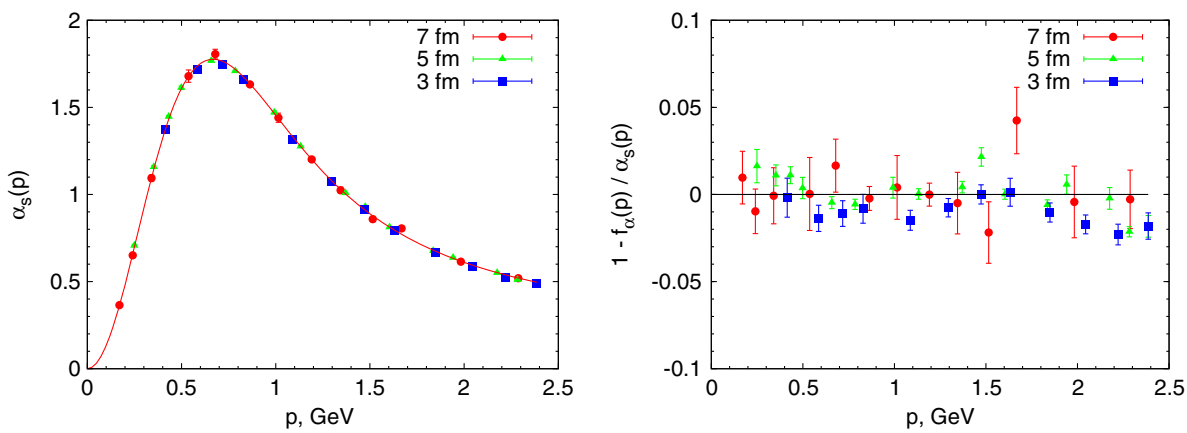

FIG. 6 (color online). Left: The momentum dependence of the running coupling for three different lattice sizes at $\beta = 2.3$. The curve shows a fit with Eq. (19) for $aL \simeq 7$ fm. Right: The relative deviation of the data for the running coupling $\alpha_s(p)$ from the fitting curve.

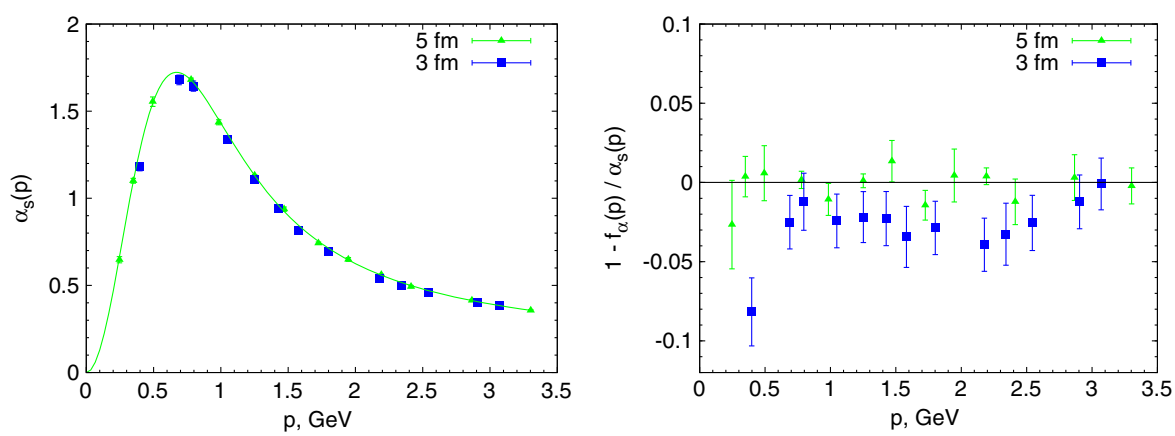

FIG. 7 (color online). Same as in Fig. 6 but for two lattice sizes at $\beta = 2.4$. The curve shows the fit result with Eq. (19) for $aL \simeq 5$ fm.

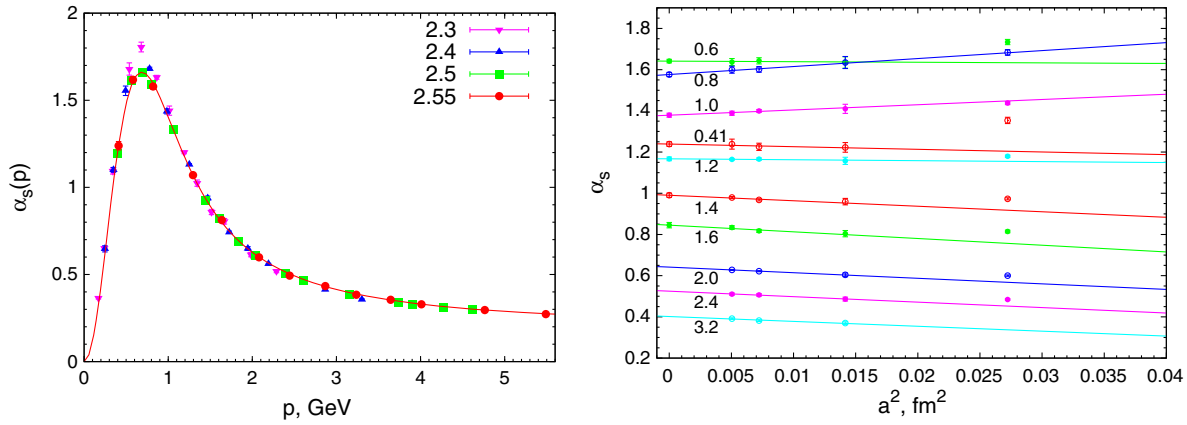

FIG. 8 (color online). Left: The momentum dependence of the running coupling for four different β-values or lattice spacings at lattice extent $aL \simeq 3$ fm. The curve shows the fit result with Eq. (19) for $\beta = 2.55$. Right: The extrapolation to the continuum limit with a function linear in a^2 for selected momenta (in GeV).

limit for selected momenta. The running coupling for these selected momenta as a linear function of a^2 is shown in the right panel of Fig. 8 together with extrapolations to the $a = 0$ limit. One can see that finite lattice spacing effects are very strong at $\beta = 2.3$. The respective data were not included into the continuum extrapolation. Another feature seen from this figure is that the sign of the scaling violation effects changes twice: it is negative to the left from the maximum of $\alpha_s(p)$ ($p = 0.41$ and 0.6 GeV), becomes positive right above it ($p = 0.8$ and 1.0 MeV) and then again turns negative. In the range of momenta $p >$ 1.2 GeV the effect is rather stable in strength up to our maximal momentum value.

In Fig. 9 we present our results for the continuum values of the running coupling $\alpha_s(p)$ for linear size $aL \simeq 3$ fm. For the fit the same *ansatz* according to Eq. (19) was used. The fit parameters are included in Table III (as the last line).

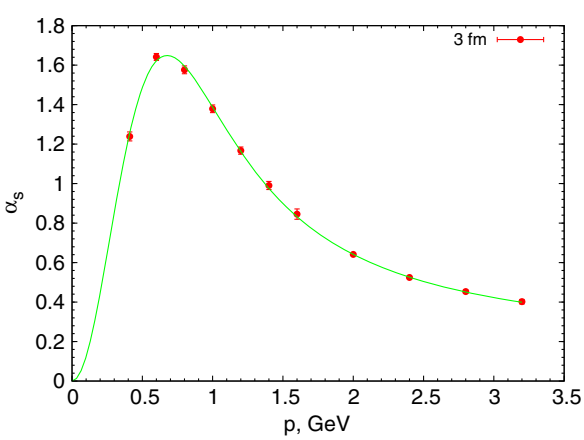

FIG. 9 (color online). The momentum dependence of the running coupling $\alpha_s(p)$ extracted in the continuum limit for selected momenta and $aL \simeq 3$ fm. The curve shows a fit corresponding to the *ansatz* Eq. (19).

Since the running coupling α_s seems to tend to zero in the IR limit, our results obtained within the framework of Landau gauge fixing as described above are fully compatible with the IR-decoupling scenario discussed in the context of the Dyson-Schwinger and functional renormalization group approach [20,79].

V. CONCLUSIONS

Completing an earlier work [70] we have computed the Landau gauge ghost dressing function for lattice $SU(2)$ pure gauge theory. In combination with the former results for the gluon propagator we have now presented the running coupling in the minimal MOM scheme. We have employed the same sets of gauge-fixed field configurations as analyzed in [70]. They had been obtained with a gauge fixing method consisting of a combined application of $Z(2)$-flips and repeated simulated annealing with subsequent overrelaxation for the gauge functional. This method was used in order to get as close as possible to the fundamental modular region i.e. to the global extremum of the gauge functional, by choosing among $\mathcal{O}(50\text{–}80)$ copies. It previously was suggested to provide a possible solution for the Gribov problem with suppressed finite size effects [75,77].

Assuming that the Gribov problem is kept under control to the best of our present knowledge, we concentrated ourselves on systematic effects like finite size and lattice spacing dependences. While finite size effects were confirmed to be rather small, the lattice spacing artifacts turned out to be non-negligible as well for the renormalized ghost dressing function as for the running coupling. In both cases for a linear lattice size of approximately $aL \simeq 3$ fm (and for the ghost dressing function with a subtraction momentum of $\mu = 2.2$ GeV) we have seen relative deviations at $\beta = 2.30$ from the results obtained at our largest $\beta = 2.55$ reaching a ten percent level at the lowest accessible momentum values and still around five percent in the

nonperturbative region around 1 GeV. This tells us that lattice results for Landau gauge gluon and ghost propagators in this momentum range have still to be taken with some caution concerning the Gribov problem and the continuum limit.

Consequently we tried an extrapolation to the continuum limit for the $aL \simeq 3$ fm volume, where we could rely on several values of the lattice spacing. We did this with fixed physical momenta chosen between 0.41 and 3.2 GeV. We presented fit formulas for the continuum limit of the ghost dressing function as well as of the running coupling valid in this range. For momenta above 0.6 GeV we have seen that also finite volume effects are under control.

Although the ghost dressing function in the restricted momentum range has been equally well fitted by a weakly IR singular behavior [see Eq. (16)] or with an IR regular *ansatz* Eq. (17), thus leaving open an IR finite limit, the result for the running coupling $\alpha_s(p)$ turned out to be robust, which emphasizes the compatibility with the infrared *decoupling solution* of Dyson-Schwinger and functional renormalization group equations.

ACKNOWLEDGMENTS

This investigation has been partly supported by the Heisenberg-Landau program of collaboration between the Bogoliubov Laboratory of Theoretical Physics of the Joint Institute for Nuclear Research Dubna (Russia) and German institutes and partly by the DFG Grant No. Mu 932/7-1. V. G. B. acknowledges support by RFBR Grant No. 11-02-01227-a and jointly with V. K. M. by RFBR Grant No. 13-02-01387-a.

[1] V. N. Gribov, Nucl. Phys. **B139**, 1 (1978).
[2] T. Kugo and I. Ojima, Prog. Theor. Phys. Suppl. **66**, 1 (1979).
[3] D. Zwanziger, Nucl. Phys. **B364**, 127 (1991).
[4] D. Zwanziger, Phys. Rev. D **65**, 094039 (2002).
[5] D. Zwanziger, arXiv:0904.2380.
[6] L. von Smekal, R. Alkofer, and A. Hauck, Phys. Rev. Lett. **79**, 3591 (1997).
[7] L. von Smekal, A. Hauck, and R. Alkofer, Ann. Phys. (N.Y.) **267**, 1 (1998).
[8] R. Alkofer and L. von Smekal, Phys. Rep. **353**, 281 (2001).
[9] R. Alkofer, C. S. Fischer, and L. von Smekal, Eur. Phys. J. A **18**, 261 (2003).
[10] C. S. Fischer and R. Alkofer, Phys. Lett. B **536**, 177 (2002).
[11] C. S. Fischer, R. Alkofer, and H. Reinhardt, Phys. Rev. D **65**, 094008 (2002).
[12] J. M. Pawlowski, D. F. Litim, S. Nedelko, and L. von Smekal, Phys. Rev. Lett. **93**, 152002 (2004).
[13] R. Alkofer, C. S. Fischer, and F. J. Llanes-Estrada, Phys. Lett. B **611**, 279 (2005).
[14] C. S. Fischer and J. M. Pawlowski, Phys. Rev. D **75**, 025012 (2007).
[15] P. Boucaud, J. P. Leroy, A. Le Yaouanc, A. Y. Lokhov, J. Micheli, O. Pene, J. Rodriguez-Quintero, and C. Roiesnel, Eur. Phys. J. A **31**, 750 (2007).
[16] P. Boucaud, J.-P. Leroy, A. L. Yaouanc, J. Micheli, O. Pene, and J. Rodriguez-Quintero, J. High Energy Phys. 06 (2008) 012.
[17] P. Boucaud, J. P. Leroy, A. Le Yaouanc, J. Micheli, O. Pene, and J. Rodriguez-Quintero, J. High Energy Phys. 06 (2008) 099.
[18] A. C. Aguilar, D. Binosi, and J. Papavassiliou, Phys. Rev. D **78**, 025010 (2008).
[19] M. Pennington and D. Wilson, Phys. Rev. D **84**, 119901 (2011).
[20] C. S. Fischer, A. Maas, and J. M. Pawlowski, Ann. Phys. (Amsterdam) **324**, 2408 (2009).
[21] J. Braun, H. Gies, and J. M. Pawlowski, Phys. Lett. B **684**, 262 (2010).
[22] D. Dudal, S. P. Sorella, N. Vandersickel, and H. Verschelde, Phys. Rev. D **77**, 071501 (2008).
[23] D. Dudal, J. A. Gracey, S. P. Sorella, N. Vandersickel, and H. Verschelde, Phys. Rev. D **78**, 065047 (2008).
[24] R. Alkofer, Braz. J. Phys. **37**, 144 (2007).
[25] G. Eichmann, I. C. Cloet, R. Alkofer, A. Krassnigg, and C. D. Roberts, Phys. Rev. C **79**, 012202 (2009).
[26] A. Sternbeck, K. Maltman, M. Müller-Preussker, and L. von Smekal, *Proc. Sci.*, LATTICE2012 (2012) 243 [arXiv:1212.2039].
[27] F. Burger, V. Lubicz, M. Müller-Preussker, S. Simula, and C. Urbach, Phys. Rev. D **87**, 034514 (2013).
[28] K. G. Chetyrkin, Nucl. Phys. **B710**, 499 (2005).
[29] K. G. Chetyrkin and A. Maier, J. High Energy Phys. 01 (2010) 092.
[30] J. E. Mandula and M. Ogilvie, Phys. Lett. B **185**, 127 (1987).
[31] H. Suman and K. Schilling, Phys. Lett. B **373**, 314 (1996).
[32] D. B. Leinweber, J. I. Skullerud, A. G. Williams, and C. Parrinello (UKQCD Collaboration), Phys. Rev. D **60**, 094507 (1999).
[33] D. Becirevic, P. Boucaud, J. P. Leroy, J. Micheli, O. Pene, J. Rodriguez-Quintero, and C. Roiesnel, Phys. Rev. D **60**, 094509 (1999).
[34] D. Becirevic, P. Boucaud, J. P. Leroy, J. Micheli, O. Pene, J. Rodriguez-Quintero, and C. Roiesnel, Phys. Rev. D **61**, 114508 (2000).
[35] F. D. R. Bonnet, P. O. Bowman, D. B. Leinweber, and A. G. Williams, Phys. Rev. D **62**, 051501 (2000).
[36] F. D. R. Bonnet, P. O. Bowman, D. B. Leinweber, A. G. Williams, and J. M. Zanotti, Phys. Rev. D **64**, 034501 (2001).

[37] J. C. R. Bloch, A. Cucchieri, K. Langfeld, and T. Mendes, Nucl. Phys. B, Proc. Suppl. **119**, 736 (2003).
[38] J. C. R. Bloch, A. Cucchieri, K. Langfeld, and T. Mendes, Nucl. Phys. **B687**, 76 (2004).
[39] S. Furui and H. Nakajima, Phys. Rev. D **69**, 074505 (2004).
[40] P. Boucaud, J. P. Leroy, A. Le Yaouanc, A. Y. Lokhov, J. Micheli, O. Pene, J. Rodriguez-Quintero, and C. Roiesnel, Phys. Rev. D **72**, 114503 (2005).
[41] A. Sternbeck, E.-M. Ilgenfritz, M. Müller-Preussker, and A. Schiller, Phys. Rev. D **72**, 014507 (2005).
[42] P. O. Bowman, U. M. Heller, D. B. Leinweber, M. B. Parappilly, A. Sternbeck, L. von Smekal, A. G. Williams, and J. Zhang, Phys. Rev. D **76**, 094505 (2007).
[43] A. Cucchieri and T. Mendes, *Proc. Sci.*, LAT2007 (2007) 297 [arXiv:0710.0412].
[44] A. Cucchieri and T. Mendes, Phys. Rev. Lett. **100**, 241601 (2008).
[45] A. Cucchieri, T. Mendes, O. Oliveira, and P. Silva, Phys. Rev. D **76**, 114507 (2007).
[46] A. Sternbeck, L. von Smekal, D. B. Leinweber, and A. G. Williams, *Proc. Sci.*, LAT2007 (2007) 340 [arXiv:0710.1982].
[47] A. Cucchieri and T. Mendes, Phys. Rev. D **78**, 094503 (2008).
[48] O. Oliveira and P. J. Silva, Phys. Rev. D **79**, 031501 (2009).
[49] I. L. Bogolubsky, E.-M. Ilgenfritz, M. Müller-Preussker, and A. Sternbeck, Phys. Lett. B **676**, 69 (2009).
[50] O. Oliveira and P. J. Silva, Phys. Rev. D **86**, 114513 (2012).
[51] A. Maas, Phys. Rev. D **91**, 034502 (2015).
[52] A. Cucchieri, Nucl. Phys. **B508**, 353 (1997).
[53] T. D. Bakeev, E.-M. Ilgenfritz, V. K. Mitrjushkin, and M. Müller-Preussker, Phys. Rev. D **69**, 074507 (2004).
[54] S. Furui and H. Nakajima, AIP Conf. Proc. **717**, 685 (2004).
[55] P. J. Silva and O. Oliveira, Nucl. Phys. **B690**, 177 (2004).
[56] S. Furui and H. Nakajima, Phys. Rev. D **70**, 094504 (2004).
[57] I. L. Bogolubsky, G. Burgio, V. K. Mitrjushkin, and M. Müller-Preussker, Phys. Rev. D **74**, 034503 (2006).
[58] V. G. Bornyakov, V. K. Mitrjushkin, and M. Müller-Preussker, Phys. Rev. D **79**, 074504 (2009).
[59] A. Maas, Phys. Rev. D **79**, 014505 (2009).
[60] A. Maas, J. M. Pawlowski, D. Spielmann, A. Sternbeck, and L. von Smekal, Eur. Phys. J. C **68**, 183 (2010).
[61] C. Hughes, D. Mehta, and J.-I. Skullerud, Ann. Phys. (Amsterdam) **331**, 188 (2013).
[62] A. Maas, Phys. Lett. B **689**, 107 (2010).
[63] A. Sternbeck and M. Müller-Preussker, Phys. Lett. B **726**, 396 (2013).
[64] D. Zwanziger, Phys. Rev. D **87**, 085039 (2013).
[65] A. Cucchieri, D. Dudal, and N. Vandersickel, Phys. Rev. D **85**, 085025 (2012).
[66] L. von Smekal, A. Jorkowski, D. Mehta, and A. Sternbeck, *Proc. Sci.*, CONFINEMENT8 (2008) 048 [arXiv:0812.2992].
[67] G. Burgio, M. Quandt, and H. Reinhardt, Phys. Rev. D **81**, 074502 (2010).
[68] A. Cucchieri, D. Dudal, T. Mendes, and N. Vandersickel, Phys. Rev. D **90**, 051501 (2014).
[69] A. Cucchieri, D. Dudal, T. Mendes, and N. Vandersickel, *Proc. Sci.*, LATTICE2014 (2014) 347 [arXiv:1410.8410].
[70] V. G. Bornyakov, V. K. Mitrjushkin, and M. Müller-Preussker, Phys. Rev. D **81**, 054503 (2010).
[71] L. von Smekal, K. Maltman, and A. Sternbeck, Phys. Lett. B **681**, 336 (2009).
[72] D. Zwanziger, Nucl. Phys. **B412**, 657 (1994).
[73] J. Fingberg, U. M. Heller, and F. Karsch, Nucl. Phys. **B392**, 493 (1993).
[74] B. Lucini and M. Teper, J. High Energy Phys. 06 (2001) 050.
[75] I. L. Bogolubsky, V. G. Bornyakov, G. Burgio, E.-M. Ilgenfritz, V. K. Mitrjushkin, and M. Müller-Preussker, Phys. Rev. D **77**, 014504 (2008).
[76] P. Schemel, Diploma thesis, Humboldt University, Berlin, Germany, 2006 [http://pha.physik.hu-berlin.de] -Theses.
[77] I. L. Bogolubsky, V. G. Bornyakov, G. Burgio, E.-M. Ilgenfritz, V. K. Mitrjushkin, M. Müller-Preussker, and P. Schemel, *Proc. Sci.*, LAT2007 (2007) 318 [arXiv:0710.3234].
[78] Y. Nakagawa, A. Voigt, E.-M. Ilgenfritz, M. Müller-Preussker, A. Nakamura, T. Saito, A. Sternbeck, and H. Toki, Phys. Rev. D **79**, 114504 (2009).
[79] P. Boucaud, J. P. Leroy, A. L. Yaouanc, J. Micheli, O. Pene, and J. Rodriguez-Quintero, Few-Body Syst. **53**, 387 (2012).